Use of a Chemical-Looping Reaction to Determine the Residence Time Distribution of Solids in a Circulating Fluidized Bed

Felix Donat,*[a] Wenting Hu,[b] Stuart A. Scott,[b] and John S. Dennis[a]

The residence time distribution (RTD) of solids in various sections of a circulating fluidized bed (CFB) is of great importance for design and operation but is often difficult to determine experimentally. A noninvasive method is described, for which the RTD was derived from temporal measurements of the temperature following the initiation of a chemical-looping reaction. To demonstrate the method, a CuO-based oxygen carrier was used in a small-scale CFB, and measurements were made in the fuel reactor, operated as a bubbling fluidized bed. The measurements were fitted to the tanks-in-series model, modified to account for heat losses from the reactor. There was excellent agreement between the model and the experiment. Limitations and further improvements of the method are discussed, also with respect to larger reactors.

Introduction

Chemical looping offers the possibility of intrinsic separation of CO_2 from a combustion process in which it is desired to capture CO_2 and bury it in the earth to prevent its release to the atmosphere. In its basic form, gaseous fuel is oxidized by a solid metal oxide, MeO, the "oxygen carrier" (OC), in one reactor [Eq. (1)]:

$$(2n+m)\,MeO_y + C_nH_{2m} \rightarrow$$
$$(2n+m)\,MeO_{y-1} + m\,H_2O + n\,CO_2 \quad (1)$$
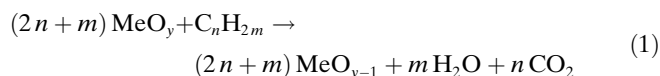
The exit gas yields almost-pure CO_2 if the steam is condensed. The reduced metal oxide, MeO_{y-1}, is transferred to an oxidation reactor and regenerated [Eq. (2)]:

$$MeO_{y-1} + air \rightarrow MeO_y \quad (2)$$

Adding these reactions, the fuel has been combusted, but the resulting CO_2 has been separated from the nitrogen in the air. This approach is generally considered to require much less energy than other techniques mooted for the capture of carbon, such as scrubbing flue gases by using amine solvents.[1] With solid fuels, the general strategy is to gasify the fixed carbon in the solid to synthesis gases, which in turn react with the OC. Practically, chemical-looping combustion (CLC) is achieved in a continuous process by circulating the solid OC between two reactors, one called the fuel reactor (FR), in which the combustion of the carbonaceous fuel takes place, and another called the air reactor (AR), in which the oxidation of the reduced OC takes place.

Oxygen carriers are key in CLC and initial investigations of the performance of newly developed OC particles usually utilize thermogravimetric analyzers, benchscale fixed bed or fluidized bed reactors.[2–8] It has, however, been shown that these types of equipment are not sufficient to emulate the reaction conditions experienced by the particles in continuously operating reactors.[9,10] Circulating fluidized bed (CFB) technology is commonly employed in these systems, in which mechanical stresses experienced by the OC particles are significantly greater than in, for example, batch fluidized bed reactors.[11] It is therefore essential to evaluate the suitability of new materials and formulations in the laboratory by using reactors capable of reproducing features of large reactors.[12–15] Not only can they be used to investigate new carrier materials, but they can also be used to investigate the process conditions, for example, the impact of sulfurous or nitrogenous species.[16,17] Most importantly, if designed carefully, small-scale systems can emulate larger reactors,[18–21] which allows the results from the laboratory to be used for the modeling of large-scale systems.

One important item of information required of scaled-down systems is the residence time distribution (RTD) of the

[a] F. Donat, Prof. J. S. Dennis
Department of Chemical Engineering and Biotechnology
University of Cambridge
Pembroke Street, Cambridge, CB2 3RA (UK)
E-mail: fd299@cam.ac.uk

[b] Dr. W. Hu, Dr. S. A. Scott
Department of Engineering
University of Cambridge
Trumpington Street, Cambridge, CB2 1PZ (UK)

This publication is part of a Special Issue on "Chemical Looping Technologies". A link to the issue's Table of Contents will appear here once it is complete.

These are not the final page numbers! ↗↗

carrier particles in the AR and the FR. Whilst operating at steady state in a CFB, only the mean residence time, t_m, of the particles in the respective reactor, rather than the RTD, is required to predict both conversion and off-gas concentrations. In most cases, t_m can be approximated reasonably well by the space time, that is, the inventory of a reactor divided by the rate of circulation of the particles. However, to understand how carrier particles evolve over time in a system of coupled reactors and to understand mixing characteristics in various parts of the reactor quantification of the RTD is required. This information may also be helpful to improve the design of the reactor. Various methods have been proposed to measure the RTD of solids in a CFB,[22,23] many of which are invasive, require a tracer, lack closed boundary conditions, or need to be performed at temperatures different from the desired process conditions. The present paper describes a noninvasive method, in which the RTD was derived from excursions in temperature following the initiation of the looping reaction. The experiments used a CuO-based OC and were undertaken in a laboratory-scale CFB.

Description of the Experiment

The principal idea is that the initiation of the looping reaction, for example, the oxidation of the OC in the AR or the reduction of the OC in the FR, results in a gradual change in temperature related to the enthalpy of the reaction. From observations of the change in temperature with time, the RTD of the OC particles can be determined, as follows. Eventually (after a time $\gg t_m$), a steady state will be reached. The reaction can be initiated by switching the fluidizing gas from an inert gas to a reactive gas. This is discussed exemplarily for the FR, which was operated as a gently bubbling fluidized bed ($U_0/U_{mf} \approx 2$–4, in which U_0 is the superficial gas velocity and U_{mf} is the minimum fluidization velocity), and for which the temperature was measured near the solids outlet approximately 5 mm from the wall of the reactor of diameter 40 mm. The electrically heated CFB is described in the Experimental Section and is depicted in Figure 3. The residence time of the gas was small relative to that of the solids and is thus not discussed.

Theory

The reduction of CuO to Cu is generally fast, even at temperatures as low as approximately 250–300 °C.[24–26] For example, with 10 vol% CO in N_2 as the reducing gas into the FR

under bubbling conditions in an initial experiment, no CO was detected in the off-gas for temperatures greater then approximately 220 °C. To measure the RTD of the particles, the CFB was operated at approximately 400 °C at ambient pressure, and consequently, the rate of reduction of the OC in the FR was most probably limited by interphase transfer of mass from the bubble to the particulate phase. Under such conditions, there was no dependence of rate on conversion, X, of the OC particles ($X=0$ implies the OC was fully oxidized, $X=1$ implies the OC was fully reduced) and X was rather low. Under typical operating conditions (summarized in Table 1) the maximum X at steady state was between 0.006 and 0.021.

The amount of heat, Q_{tot}, produced from the reaction over the duration that reactive gas was fed to the FR was [Eq. (3)]:

$$Q_{tot} \cdot C_{in}(t) = 2\, n_{O_2,tot} \cdot C_{in}(t) \cdot \Delta H_{r,400\,°C} \tag{3}$$

in which C_{in} is a normalized input vector (e.g., a rectangular function with unit area for the duration of the reactive gas turned on), $n_{O_2,tot}$ is the equivalent total number of moles of O_2 transferred from the OC particles to the CO, and $\Delta H_{r,400°C}$ is the enthalpy of the reaction. The value of $n_{O_2,tot}$ was calculated by using [Eq. (4)]:
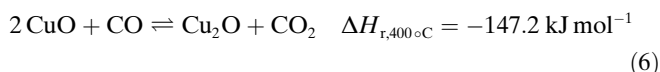
$$n_{O_2,tot} = 0.5 \cdot \int_{t_0}^{\infty} x_{CO,in} \cdot \dot{V}_{FR} \cdot \frac{p}{R \cdot T} \cdot dt \tag{4}$$

in which $x_{CO,in}$ is the mole fraction of CO in the fuel gas; $\dot{V}_{FR}$ is the flow rate of gas entering the FR [$m^3 s^{-1}$], measured at ambient pressure and temperature (taken as $p=101\,325$ Pa and $T=293$ K); R is the gas constant; and t_0 is the time at which the reactive gas was admitted to the reactor. A very diluted fuel gas ($x_{CO,in}=0.1$) was used 1) to limit the increase in temperature during the exothermic reduction of CuO to avoid significant influences on the hydrodynamics, 2) to limit the conversion of CuO to avoid significant changes in the physical properties of the particles, and 3) to ensure the thermodynamic properties of the fluidizing gas in the FR did not change unduly.

At a temperature of 400 °C, CuO is known to preferentially reduce to Cu directly, with only small amounts of Cu_2O being formed as an intermediate.[26,27] Thus, for low values of X, the reduction of CuO by CO can be written as [Eqs. (5) and (6)]:

Table 1. Summary of the experimental conditions used for runs 1–4 at approximately 400 °C, and the modeling parameters obtained from the best fit of Equations (9)—(12) to the temperature measured in the FR.

Exp.	$\dot{V}_{FR}$ [$m^3 s^{-1}$]	ε_{FR}	$\dot{m}_s$ [$g\,s^{-1}$]	$m_{FR}/\dot{m}_s$	N	k [$W\,K^{-1}$]	Q_{loss} [$J\,K^{-1}$]	t'_m [s]	t_m [s]
1	6×10^{-5}	0.57	1.8	54	1.4	0.75	160	108	54
2	5×10^{-5}	0.55	1.3	79	1.4	0.9	150	119	78
3	5×10^{-5}	0.55	4.6	22	1.35	−0.35	215	88	22
4	6.5×10^{-5}	0.58	2.4	40	1.4	0.35	165	103	39

$$CuO + CO \rightleftharpoons Cu + CO_2 \quad \Delta H_{r,400\,°C} = -130.2\,kJ\,mol^{-1} \tag{5}$$

$$2\,CuO + CO \rightleftharpoons Cu_2O + CO_2 \quad \Delta H_{r,400\,°C} = -147.2\,kJ\,mol^{-1} \tag{6}$$

Autothermal operation is usually not possible in small-scale CFBs. If the circulation of solids in the CFB (in the absence of a chemical reaction in the FR) reaches a steady state, the heat transferred from the heating elements to the CFB (including the heating of the gas and the solids) and the heat losses from the CFB are eventually in balance. The enthalpies of reaction per mole of CO are relatively similar for reactions (5) and (6). Because reaction (5) is dominant, a value of $\Delta H_{r,400\,°C}$ of $-130.2\,kJ\,mol^{-1}$ was used in subsequent calculations.

Heat is generated at the gas–solid interface and is then transferred to the gas, the surface of the particles, and from there to the interior of the particles. It was previously shown that heat transfer by conduction inside an OC particle is generally fast, so that internal gradients of temperature are insignificant.[28] It was additionally shown that the main resistance for heat transfer is in the external film of the particles, which affects the increase in temperature of a particle in the first few seconds of a reaction (simulated for fuel gas concentrations of 70 vol%). Given the low value of $x_{CO,in}$, the high porosity of the particles, and the rather long timescale of the reaction ($t > t_m$, see below), any effects of heat-transfer resistance on the measurements can safely be ruled out, including those to the thermocouple. Treating the enthalpy of reaction as a heat input to the system (i.e., the reaction occurs only close to the inlet), as a first approximation assuming no heat loss, the heat balance for the FR yields, as shown in the Supporting Information [Eq. (7)]:

$$T(t) - T_0 = \frac{[Q_{tot} \cdot C_{in}(t)]^*E'(t)}{c_{p,s} \cdot \dot{m}_s + c_{p,g} \cdot \dot{V}_{FR} \cdot \rho_g} \tag{7}$$

in which * is the convolution operator, $c_{p,s}$ is the specific heat capacity of the solids, $E'(t)$ is the response to an impulse of heat input, T_0 is the temperature just before the initiation of the reduction reaction, T is the temperature measured near the outlet of the FR, $c_{p,g}$ is the specific heat capacity of the fluidizing gas, and ρ_g is the density of the fluidizing gas. The OC consisted of 60 wt% CuO, 23 wt% Al_2O_3, and 17 wt% CaO, which gave a value of $c_{p,s}$ of approximately 808 $J\,kg^{-1}\,K^{-1}$ at 400 °C.[29] This value changed insignificantly over the temperature range investigated in this work [($\approx 400 \pm 20$) °C] and was used for the solids both entering and leaving the FR. The heat transferred to the gas is small relative to that to the solids, so that the corresponding term on the right-hand side of Equation (7) can be neglected, which then gives [Eq. (8)]:

$$T(t) - T_0 = \frac{Q_{tot} \cdot [C_{in}(t)^*E'(t)]}{c_{p,s} \cdot \dot{m}_s} \tag{8}$$

Modeling the RTD of the solids

The tanks-in-series (TIS) model with the gamma extension model[30,31] was used to model the RTD of the solids. The TIS model was used successfully in previous RTD studies of fluidized beds.[32–36] It assumes that the system of interest consists of N statistically independent tanks of equal volume in series and that the solids in each tank are perfectly mixed. For $N \to \infty$, the E curve obtained by the model approaches that of a plug flow reactor. The RTD, $E(t)$, is therefore [Eq. (9)]:[31]

$$E(t) = \frac{t^{N-1}}{t_m^N} \cdot \frac{N^N}{\Gamma(N)} \cdot e^{-\frac{t \cdot N}{t_m}} \tag{9}$$

in which $\Gamma(N)$ is the gamma function and N can be any rational number > 0 [Eq. (10)]:

$$\Gamma(N) = \int_{x=0}^{\infty} e^{-x} \cdot x^{N-1} \cdot dx \tag{10}$$

Of course, the parameter N lacks physical interpretation; rather, N should be considered as an adjustable index of mixing performance.[31] For the model to be used in the heat balance, Equation (8) needs to be modified to account for losses of heat from the reactor; otherwise, $E(t)$ would give a "heat RTD", rather than a "material RTD" related to the physical mixing of the particles. In the modified TIS model, derived in the Supporting Information, heat is lost as particles flow from one virtual tank to another, as shown in Figure S1 (Supporting Information), and is quantified by the parameter k [$W\,K^{-1}$], related to the temperature of each tank. Additionally, heat is transferred to the reactor, quantified by the parameter Q_{loss} [$J\,K^{-1}$], and is assumed to be uniform over time. Thus, Equation (8) becomes [Eq. (11)]:

$$T(t) - T_0 = \left(\frac{c_{p,s} \cdot \dot{m}_s}{c_{p,s} \cdot \dot{m}_s + k}\right)^N \cdot \frac{Q_{tot} \cdot [C_{in}(t)^*E'(t)]}{c_{p,s} \cdot \dot{m}_s} \tag{11}$$

in which the parameter t_m from Equation (9) is written as [Eq. (12)]:

$$t'_m = \frac{m_{FR} \cdot c_{p,s} + Q_{loss}}{c_{p,s} \cdot \dot{m}_s + k} \tag{12}$$

In this model, $E'(t)$ should have the same value of N as $E(t)$, the RTD of the solids, but with a different time constant. The inventory of solids in the FR was [Eq. (13)]:

$$m_{FR} = \rho_s \cdot A_{FR} \cdot h \cdot (1 - \varepsilon_{FR}) \tag{13}$$

in which the bed voidage, ε_{FR}, is estimated from the two-phase assumption,[37] A_{FR} is the cross-sectional area of the FR, and h is the height of the solids in the FR (0.1 m). The method of least squares was used to fit Equations (9)–(12) to the measured temperature, for which k, N, and Q_{loss} were the three fitting parameters. It is noteworthy that the TIS model itself is a one-parameter model, and so the parameter N is sufficient to characterize the mixing of the solids in the reactor.[31] On the basis of t'_m, the true mean residence time of the solids, t_m, can be derived from [Eq. (14)]:

$$t_m = t'_m \cdot \frac{c_{p,s} \cdot \dot{m}_s + k}{c_{p,s} \cdot \dot{m}_s} - \frac{Q_{loss}}{c_{p,s} \cdot \dot{m}_s} \quad (14)$$

Results

Figure 1 shows an example of the excursion in temperature measured in the FR following the initiation of the exothermic reduction reaction by switching the fluidizing gas from N_2 to 10 vol% CO in N_2 in comparison to that modeled by
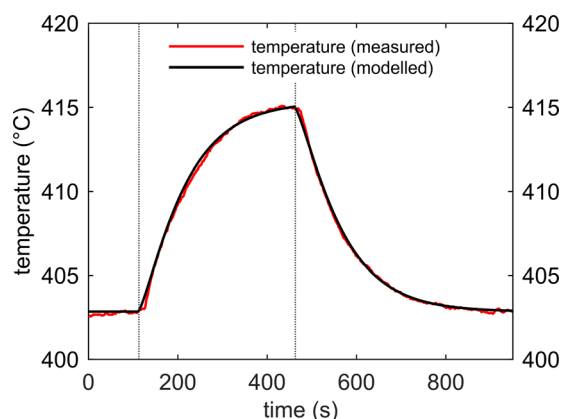

Figure 1. Temperature in the FR as a function of time, following the initiation of the reduction of the OC particles by CO. The red line corresponds to the measured temperature. The black line was computed by using Equation (11) with $N = 1.4$, $k = 0.75$ W K^{-1}, $Q_{loss} = 160$ J K^{-1}, and $t'_m = 108$ s. The reactive gas was turned on for a total of 350 s, indicated by the vertical dashed lines.

using Equation (11). The flow rate of gas remained the same, here $\dot{V}_{FR} = 6 \times 10^{-5}$ m^3 s^{-1}, which resulted in a value of U_0/U_{mf} of approximately 3. The bed voidage was $\varepsilon_{FR} = 0.57$, and the inventory of the FR was $m_{FR} = 0.097$ kg. Excellent agreement between the two curves was obtained for $N = 1.4$, $k = 0.75$ W K^{-1}, and $Q_{loss} = 160$ J K^{-1}, which gave $t'_m = 108$ s. Small deviations were found in the first few seconds after the reactive gas was switched on and off. Using Equation (14), t_m was calculated to be 53.7 s. This value compares well to the space time ($m_{FR}/\dot{m}_s$) of 54.1 s, consistent with the system having closed boundaries (i.e., each particle passes the system boundaries exactly twice; the first time upon entering the FR and the second time upon leaving the FR by the overflow).

Additional measurements (experiments 2–4) were made by using different flow rates $\dot{V}_{FR}$ and solids circulation rates $\dot{m}_s$, as summarized in Table 1. The best fit for these measure-

ments gave values of N between 1.35 and 1.4, which indicated that $\dot{V}_{FR}$ and $\dot{m}_s$ did not affect N significantly. The values of Q_{loss} varied only slightly with the estimated space time, whereas k changed considerably; this is discussed in greater detail below.

The RTDs corresponding to the fitted temperature curves for experiments 1–4 are shown in Figure 2. For the computation of the E curves, N and t_m were used in Equation (9). It is clear that the shape of the RTD was similar for each experiment, subject to the individual values of t_m.
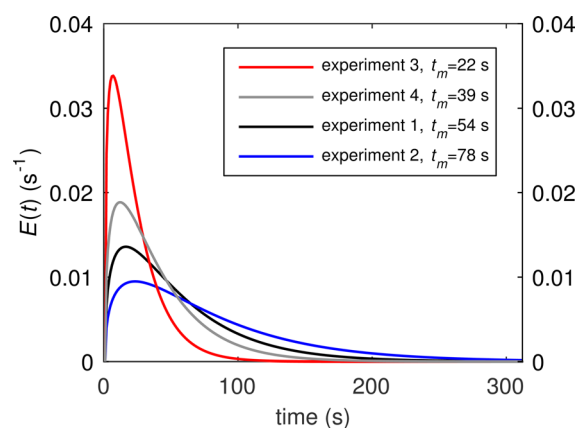
Figure 2. Comparison of the computed E curves for the four experiments by using the parameters t_m and N.

Discussion

The measurement of the RTD on the basis of the temperature excursion at the exit of the FR (or AR) is dependent on the solids as dominant carriers for heat. Other terms affecting the shape of the RTD include heat transfer to the reactor body, heat loss to the surroundings, and dissipation of heat by the gas, and these are more important in small-scale systems than in larger ones. Here, in a bubbling fluidized bed, the heat capacity of the gas stream leaving the reactor was always <10% of that of the circulating solids on the basis of the lowest solids circulation rate examined and did not have a significant influence on the RTD. However, care must be taken upon deducing the RTD of solids in a fast-fluidized bed, because the heat capacity of the gas would be comparable, or even higher, than that of the circulating solids, which would hence dissipate a significant proportion of the heat released from the reaction and reduce the apparent mean residence time. However, the contribution from the gas can be accounted for relatively easily by knowing the flowrate (e.g., assuming a plug flow) and can be deconvoluted from the measured RTD. On the other hand, other thermal masses, such as the reactor body, increase the thermal inertia of the FR and increase the apparent mean residence time (i.e., $t'_m > t_m$). This is especially important in small-scale systems, for which the mass of the reactor body is large relative to the content of solids, as seen in Table 1. Here, this was accounted for by introducing an additional term, Q_{loss}, in the heat balance. For larger systems, the solid carriers tend to dominate

These are not the final page numbers! ↗↗

the thermal mass, and the contribution from the reactor body would diminish. Heat losses, k, can be significant in small systems owing to the relatively large surface area per unit volume of the reactor, and autothermal operation is usually difficult. As the scale of the system increases, the proportion of heat lost would decrease, so that the heat loss term would also become less significant.

In bubbling fluidized beds operating under conditions relevant to CLC, the rate of reaction is usually limited by interphase mass transfer. In fact, the rate of the intrinsic chemical kinetics of the OC used in the FR must be at least as fast as the rate of interphase mass transfer in a bubbling bed to avoid slip of unburned combustible gases, unless very deep beds are used. Thus, a constant rate of reaction and a constant release of heat can be assumed. In fast or turbulent beds, interphase mass transfer is significantly enhanced, and the intrinsic kinetics of the OC may become more important.[38] These would have to be included in Equation (3).

The curves obtained from Equation (11) fitted the temperature measured in experiments 1–4 very well, which indicated that the TIS model and the principal assumptions were suitable for modeling of the mixing of the particles in the FR. It was expected that the values of Q_{loss} would be very similar for the four experiments, given that it reflects the heat capacity of the reactor body. In experiment 3, the value of Q_{loss} deviated from that obtained from the other experiments, the reasons for which are not clear. A trend was seen for the parameter k, which increased with mean residence time of the particles, which suggested a possible nonlinear dependence on temperature. For experiment 3 with the highest solids circulation rate (and thus the lowest mean residence time), this value became negative, which would not be possible had k a physical meaning (in which case it would be expected to be a constant). Generally, the method described in this paper relies on accurate measurements of $\dot{m}_s$. Any inaccuracies in determining $\dot{m}_s$ will affect k, and too low a value of $\dot{m}_s$ would result in too high a value of k and vice versa from the fitting of the experimental data by using Equations (11) and (12). Further experiments are needed to quantify precisely the values of Q_{loss} and k. Most importantly, in the heat balance presented in this paper, the values of k and Q_{loss} do not affect significantly the parameter N, which characterizes the shape of the RTD and thus the mixing of the solids in the reactor.

A potential problem with the current experimental arrangement is that there was only one thermocouple at a fixed location in the FR. Provided the release of heat is fast and uniform in the bed, temperature measurements at a fixed position are sufficient to obtain information on the mixing of the particles. In the small-scale CFB used in this work, the solids in the FR were relatively well mixed, evident from the small number of N. In large systems, solid mixing would probably be more complicated and heat release no longer uniform, and thus simultaneous measurements of the temperature from multiple positions within the FR would be required for accurate characterization of the RTD, but the same basic principles should still apply. The proposed method could potentially be extended to the use of solid fuels, for which the release of heat depends on the distribution and residence time of the fuel particles in the system.

Conclusions

Knowledge of the residence time distribution (RTD) of oxygen-carrier (OC) particles in a circulating fluidized bed (CFB) is of great importance, for both design and operation. RTDs are often difficult to determine experimentally. Here, a simple method was described to determine the RTD of OC particles in reactors under conditions relevant to chemical-looping combustion (CLC). The method is noninvasive and can potentially be employed in reactors up to the large pilot scale. The following conclusions were drawn:

1) The RTD of solids can be determined from measurements of the temperature in the reactor by following the initiation of a looping reaction
2) The tanks-in-series model is suitable for modeling the mixing of the solids in the present reactor
3) Factors influencing the RTD other than the circulation rate of the solids were modeled and discussed. Some factors become less important at larger scales, which thus yields more accurate measurements of the RTD of the solids

Experimental Section

Apparatus

A schematic diagram of the experimental CFB is shown in Figure 3. The CFB was made of stainless steel (Alloy 310) and was housed in a commercial furnace system (Kanthal) consisting of six heating elements rated at 1.35 kW each. The CFB was composed of two fluidized bed reactors connected through two identical loop seals. The FR consisted of a bubbling fluidized bed with an inner diameter (i.d.) of 40 mm and an operating bed height of approximately 100 mm. The solids were transported from the FR to the AR by a standpipe (SP2) and the lower loop seal (LS2). The loop seals consisted of two chambers, each of which had a height of 80 mm and a cross-sectional area of 20 mm × 20 mm. Both chambers could be aerated independently. The AR was a bubbling fluidized bed with an i.d. of 27 mm and an operating bed height of approximately 130 mm. The outlet of the AR tapered to a tube with an i.d. of 10 mm and a length of approximately 1.6 m, which acted as the riser to transport the solids upwards. At the top of the bubbling fluidized bed in the AR, secondary air could be injected to assist the transport of the particles through the riser. Downstream of the riser, the solids were recovered by a cyclone and transported to the upper standpipe (SP1) connected to the upper loop seal (LS1). Particles from LS1 entered the FR 15 mm above the distributor by tubing with an i.d. of 10 mm immersed into the bed. Both standpipes were operated in packed bed flow.

Pressure transducers (First Sensor, HDI) were in place to monitor continuously (at a frequency of 10 Hz) the pressure drop across various sections of the CFB to ensure the system operated
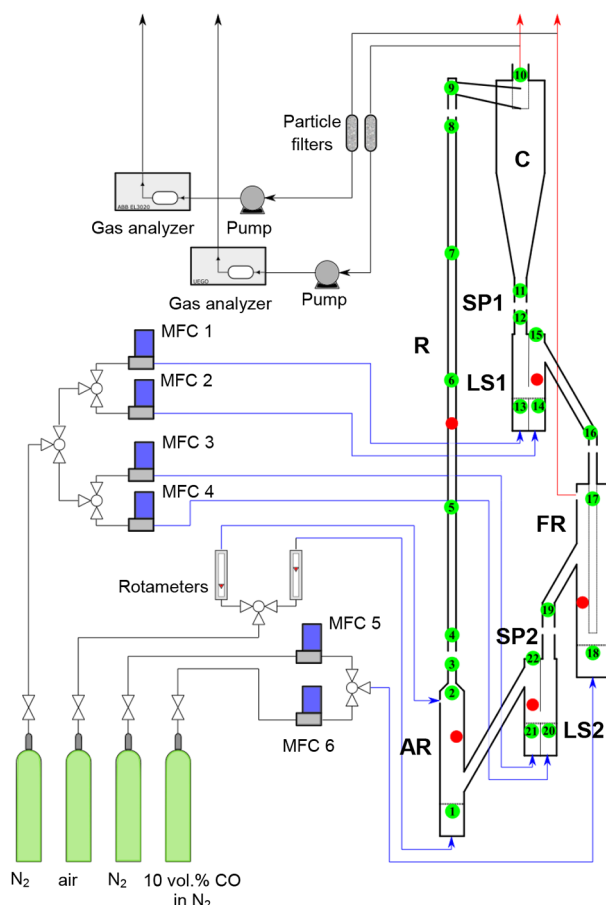
Figure 3. Schematic diagram of the experimental setup by using the CFB. AR: air reactor, C: cyclone, FR: fuel reactor, LS1: upper loop seal, LS2: lower loop seal, R: riser, SP1: upper standpipe, SP2: lower standpipe, and MFC: mass flow controller. The red circles indicate thermocouples. The green circles indicate the location of the pressure tappings (PT). The blue arrows represent the gas inlets, and the red arrows represent the gas outlets.

stably. The flow rate of gas to the loop seals and the FR was controlled by using mass flow controllers (Bronkhorst, EL-FLOW series). The flow rate of air to the AR (primary and secondary air inlet) was controlled by using rotameters (MPB Industries). The loop seals were aerated by using N_2, and the reducing gas for the purpose of measuring the RTD was 10 vol% CO in N_2. All gases other than compressed air were provided by BOC Ltd., from cylinders. The off-gases from the AR and the FR were measured continuously by using gas analyzers (Universal exhaust gas oxygen analyzer and ABB EL3020). Temperature measurements were made in the AR, the FR, the riser, and the loop seals by using type K thermocouples. The response of the thermocouples (< 1 s) was sufficiently fast and did not affect the measurements.

Measurement of the solids circulation rate

The solids circulation rate, $\dot{m}_s$, was measured in the riser of the CFB by using a method described (and validated for this system) in detail elsewhere.[39] Pressure signals associated with the passage of solids in the riser were cross-correlated to obtain an estimate of their time-averaged velocity, U_p. Simultaneously, the time-averaged voidage, ε_{riser}, was measured in the same section. The value of $\dot{m}_s$ was computed by using Equation (15):

$$\dot{m}_s = A_{riser} \cdot \rho_s \cdot (1 - \varepsilon_{riser}) \cdot U_p \qquad (15)$$

in which A_{riser} is the cross-sectional area of the riser and ρ_s is the particle density.

Materials

The CFB was operated by using approximately 300 mL of a CuO-based oxygen carrier. The OC consisted of 60 wt% CuO and 40 wt% calcium aluminate as the support material. The method of synthesis is described in detail elsewhere.[40] The OC was chosen because it performed well in previous studies,[40,41] for which it was cycled under CLC conditions in a single fluidized bed reactor at temperatures up to 950 °C. The particle density, ρ_s, was measured to be approximately 1800 kg m^{-3}, its porosity was approximately 0.65, and the mean particle diameter, d_p, (defined as the surface-volume-equivalent diameter) was approximately 220 μm. The gas velocity, U_{mf}, needed for minimum fluidization was approximately 0.036 m s^{-1} (measured at 400 °C and atmospheric pressure in air) and the bed voidage at U_{mf}, ε_{mf}, was 0.46.

[1] J. Adanez, A. Abad, F. Garcia-Labiano, P. Gayan, L. F. de Diego, *Prog. Energy Combust. Sci.* **2012**, *38*, 215–282.

[2] L. F. de Diego, F. García-Labiano, J. Adánez, P. Gayán, A. Abad, B. M. Corbella, J. M. Palacios, *Fuel* **2004**, *83*, 1749–1757.

[3] J. Adánez, L. F. de Diego, F. García-Labiano, P. Gayán, A. Abad, J. M. Palacios, *Energy Fuels* **2004**, *18*, 371–377.

[4] P. Cho, T. Mattisson, A. Lyngfelt, *Fuel* **2004**, *83*, 1215–1225.

[5] T. Mattisson, A. Järdnäs, A. Lyngfelt, *Energy Fuels* **2003**, *17*, 643–651.

[6] S. B. Peterson, G. Konya, C. K. Clayton, R. J. Lewis, B. R. Wilde, E. M. Eyring, K. J. Whitty, *Energy Fuels* **2013**, *27*, 6040–6047.

[7] Q. Imtiaz, M. Broda, C. R. Müller, *Appl. Energy* **2014**, *119*, 557–565.

[8] G. L. Schwebel, D. Filippou, G. Hudon, M. Tworkowski, A. Gipperich, W. Krumm, *Appl. Energy* **2014**, *113*, 1902–1908.

[9] M. Rydén, D. Jing, M. Källén, H. Leion, A. Lyngfelt, T. Mattisson, *Ind. Eng. Chem. Res.* **2014**, *53*, 6255–6267.

[10] P. Knutsson, C. Linderholm, *Appl. Energy* **2015**, *157*, 368–373.

[11] C. Linderholm, M. Schmitz, *J. Environ. Chem. Eng.* **2016**, *4*, 1029–1039.

[12] E. Johansson, T. Mattisson, A. Lyngfelt, H. Thunman, *Fuel* **2006**, *85*, 1428–1438.

[13] S. R. Son, S. D. Kim, *Ind. Eng. Chem. Res.* **2006**, *45*, 2689–2696.

[14] C. R. Forero, P. Gayán, L. F. de Diego, A. Abad, F. García-Labiano, J. Adánez, *Fuel Process. Technol.* **2009**, *90*, 1471–1479.

[15] L. Shen, J. Wu, Z. Gao, J. Xiao, *Combust. Flame* **2010**, *157*, 934–942.

[16] I. Adánez-Rubio, A. Abad, P. Gayán, F. García-Labiano, L. F. de Diego, J. Adánez, *Appl. Energy* **2014**, *113*, 1855–1862.

[17] H. Gu, L. Shen, Z. Zhong, X. Niu, H. Ge, Y. Zhou, S. Xiao, S. Jiang, *Chem. Eng. J.* **2015**, *264*, 211–220.

[18] M. T. Nicastro, L. R. Glicksman, *Chem. Eng. Sci.* **1984**, *39*, 1381–1391.

[19] L. R. Glicksman, M. Hyre, K. Woloshun, *Powder Technol.* **1993**, *77*, 177–199.

[20] E. Johansson, A. Lyngfelt, T. Mattisson, F. Johnsson, *Powder Technol.* **2003**, *134*, 210–217.

[21] T. Pröll, K. Rupanovits, P. Kolbitsch, J. Bolhàr-Nordenkampf, H. Hofbauer, *Chem. Eng. Technol.* **2009**, *32*, 418–424.

[22] A. T. Harris, J. F. Davidson, R. B. Thorpe, *Chem. Eng. J.* **2002**, *89*, 127–142.

[23] A. T. Harris, J. F. Davidson, R. B. Thorpe, *Chem. Eng. Sci.* **2003**, *58*, 2181–2202.

[24] S. Y. Chuang, J. S. Dennis, A. N. Hayhurst, S. A. Scott, *Proc. Combust. Inst.* **2009**, *32*, 2633–2640.

[25] S. Y. Chuang, J. S. Dennis, A. N. Hayhurst, S. A. Scott, *Chem. Eng. Res. Des.* **2011**, *89*, 1511–1523.

[26] E. A. Goldstein, R. E. Mitchell, *Proc. Combust. Inst.* **2011**, *33*, 2803–2810.

[27] J. A. Rodriguez, J. Y. Kim, J. C. Hanson, M. Pérez, A. I. Frenkel, *Catal. Lett.* **2003**, *85*, 247–254.

[28] F. García-Labiano, L. F. de Diego, J. Adánez, A. Abad, P. Gayán, *Chem. Eng. Sci.* **2005**, *60*, 851–862.

[29] National Institute of Standards and Technology (NIST), *NIST Chemistry WebBook*, *NIST Standard Reference Database Number 69*, U.S. Department of Commerce, **2016**, http://webbook.nist.gov/chemistry/.

[30] B. A. Buffham, L. G. Gibilaro, *AIChE J.* **1968**, *14*, 805–806.

[31] E. B. Nauman, B. A. Buffham, *Mixing in Continuous Flow Systems*, Wiley, Hoboken, NJ, **1983**.

[32] P. Markström, N. Berguerand, A. Lyngfelt, *Chem. Eng. Sci.* **2010**, *65*, 5055–5066.

[33] D. C. Guío-Pérez, T. Pröll, J. Wassermann, H. Hofbauer, *Ind. Eng. Chem. Res.* **2013**, *52*, 10732–10740.

[34] D. C. Guío-Pérez, T. Pröll, H. Hofbauer, *Chem. Eng. Res. Des.* **2014**, *92*, 1107–1118.

[35] M. P. Babu, Y. P. Setty, *Can. J. Chem. Eng.* **2008**, *81*, 118–123.

[36] J. S. Rao, N. V. S. Ramani, H. J. Pant, D. N. Reddy, *Indian J. Sci. Technol.* **2012**, *5*, 3746–3752.

[37] J. F. Davidson, R. Clift, D. P. Harrison, *Fluidization*, 2nd ed., Academic, San Diego, CA, **1985**.

[38] H. T. Bi, N. Ellis, I. A. Abba, J. R. Grace, *Chem. Eng. Sci.* **2000**, *55*, 4789–4825.

[39] F. Donat, *Development of a Laboratory-Scale System for Chemical Looping Combustion*, PhD Thesis, University of Cambridge, **2016**.

[40] F. Donat, W. Hu, S. A. Scott, J. S. Dennis, *Ind. Eng. Chem. Res.* **2015**, *54*, 6713–6723.

[41] W. Hu, F. Donat, S. A. Scott, J. S. Dennis, *Appl. Energy* **2016**, *161*, 92–100.

FULL PAPERS

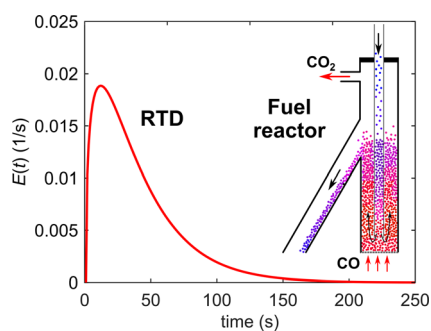*F. Donat,* W. Hu, S. A. Scott, J. S. Dennis*

■■ – ■■

Use of a Chemical-Looping Reaction to Determine the Residence Time Distribution of Solids in a Circulating Fluidized Bed

A little loopy: A noninvasive method is used to derive the residence time distribution of solids in a chemical-looping reactor. For this, a looping reaction is initiated and the increase in temperature is related to a solids mixing model, namely, the tanks-in-series model modified for effects of heat transfer.